

SUPERSONIC FLOWS AROUND BLUNTED BODIES OF SIMPLE SHAPE

**(ZATUPLENNYE TELA PROSTOI FORMY V SVERKHZVUKOVOM
POTOKE GAZA)**

PMM Vol. 24, No. 5, 1960, pp. 927-930

**P. I. CHUSHKIN
(Moscow)**

(Received 15 June 1960)

In view of the mathematical complexity of the problem of supersonic flow around blunted bodies, no sufficiently accurate analytical solutions have yet been found which are free of strong assumptions. The experimental study of the blunt-body problem is also hampered by serious difficulties (especially at high Mach numbers) and generally yields results of insufficient accuracy. Therefore, in recent times, numerical methods based on the use of high-speed computing machines have been widely applied to the problems of supersonic flow around blunted bodies. One of the most effective numerical techniques is the integral method suggested by Dorodnitsyn [1] and developed by Belotserkovskii [2,3] for two-dimensional and axisymmetric supersonic flows around blunt bodies with detached shock-waves. This method permits the construction of the mixed-flow field in the region of influence in the neighborhood of the nose of the body.

The supersonic flow downstream of that region can be computed by the method of characteristics. In the present paper, a method of characteristics, adapted to electronic computing machines, is described and applied to a series of blunted wedges and cones.

In the usual method of characteristics used in gasdynamics, the basic variables are the coordinates x , y , the Mach angle α , the angle between the local velocity vector and the x -axis θ , and the entropy s . However, in such a case, the characteristic equations contain trigonometric and exponential functions, which lead to a large number of sub-programs for the calculation of elementary functions and absorb much machine time.

Ehlers [4] suggested the use of the following unknowns in the method of characteristics:

$$\beta = \cot \alpha = \sqrt{M^2 - 1}, \quad \zeta = \tan \theta, \quad s$$

This allows the reduction of the coefficients in the characteristic equations to algebraic functions and provides substantial economy of machine time. However, the method in the form presented by Ehlers cannot be used altogether generally. (Ehlers examined only the simplest example — that of two-dimensional potential flow in a nozzle.) In Ehlers' formulation, the iterations in the computation of the shock-wave do not always converge, an unfortunate choice of the constant in the entropy function precludes computations for the case $M = \infty$ (s in the free stream was assumed zero), and no allowance was made for the possibility that the characteristic curves may be vertical or horizontal. The numerical method of characteristics, presented below for the computation of the supersonic part of flows around blunted bodies, consists of a combination of the two methods mentioned above.

For the unknown functions in this procedure we take x , y , β , ζ , and $s = \ln(p/\rho^\kappa)$, where ρ is the dimensionless density, referred to the free-stream density, ρ_∞ , p is the dimensionless pressure, referred to $\rho_\infty a_*^2$ (a_* designating the critical speed of sound), and κ is the adiabatic exponent.

Let us represent the differential equations for the characteristics and for the relationships valid along them for the first and second family in the form

$$\frac{dx}{dy} = \frac{\beta - \zeta}{\beta\zeta + 1} \equiv m, \quad d\zeta + Kd\beta + Ldy - Pds = 0 \quad (1)$$

$$\frac{dy}{dx} = \frac{\beta\zeta - 1}{\beta + \zeta} \equiv n, \quad d\zeta - Jd\beta - Ndx + Qds = 0 \quad (2)$$

where

$$J = K = -\frac{2\beta^2(\zeta^2 + 1)}{(\kappa + 1)(\beta^2 + 1)(\epsilon\beta^2 + 1)}, \quad L = j \frac{\zeta(\zeta^2 + 1)}{y(\beta\zeta + 1)}$$

$$N = j \frac{\zeta(\zeta^2 + 1)}{y(\beta + \zeta)}, \quad P = Q = \frac{\beta(\zeta^2 + 1)}{\kappa(\kappa - 1)(\beta^2 + 1)}$$

and where $j = 0$ for two-dimensional flow, $j = 1$ for axisymmetric flow, and $\epsilon = (\kappa - 1)/(\kappa + 1)$. The system (1) to (2) is written for the case where the characteristics of the first family are not horizontal and the characteristics of the second family are not vertical (with only the upper half-plane of the flow field under consideration).

The entropy s depends only on the stream-function ψ so that we may introduce a modified stream-function Ψ through the equation

$$d\Psi = (\kappa e^s)^{1/(\kappa-1)} d\psi$$

Then, we shall have along the characteristics of the second family (for example)

$$\frac{d\Psi}{dx} = -\frac{y^j \sqrt{(\beta^2 + 1)(\zeta^2 + 1)}}{(\beta + \zeta)(\epsilon\beta^2 + 1)^{1/2\epsilon}} \equiv q \tag{3}$$

The entropy s can be obtained from Ψ through the relationship $s = s(\Psi)$ established along the shock-wave.

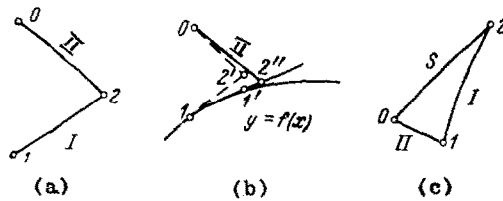


Fig. 1.

In evaluating the quantities x , y , β , ζ , Ψ , s at an arbitrary point of intersection (Fig. 1a) of a characteristic of the first family, I, and of a characteristic of the second family, II, from the corresponding known values at points 0 and 1, we apply Equations (1) to (3) in the finite-difference form. Let us write these finite-difference equations in a form similar to that of [5]:

$$x_2 = \frac{x_1 - mn x_0 + m(y_0 - y_1)}{1 - mn}, \quad y_2 = y_0 + n(x_2 - x_0) \tag{4}$$

$$\Psi_2 = \Psi_0 + q(x_2 - x_0), \quad s_2 = s(\Psi_2)$$

$$\beta_2 = \frac{\zeta_1 + K\beta_1 - L(y_2 - y_1) + P(s_2 - s_1) - \zeta_0 + J\beta_0 - N(x_2 - x_0) + Q(s_2 - s_0)}{J + K} \tag{5}$$

$$\zeta_2 = \frac{J[\zeta_1 + K\beta_1 - L(y_2 - y_1) + P(s_2 - s_1)] + K[\zeta_0 - J\beta_0 + N(x_2 - x_0) - Q(s_2 - s_0)]}{J + K}$$

This system of equations is solved by an iteration process in which the first iteration uses coefficients evaluated at points 0 or 1, respectively, and subsequent iterations use the mean values of the coefficients between the points 0 and 2, or 1 and 2. Usually three iterations suffice to give adequate accuracy. The point 2 in Fig. 1b on the body ($y = f(x)$) is computed by the iteration method described by Ehlers. In this procedure the contour is approximated by a line tangent at the point $1^i(x_1^i = x_2^i)$ in each iteration. First one finds

$$x_2 = \frac{nx_0 - y_0 + f(x_2) - x_2 f'(x_2)}{n - f'(x_2)}$$

by using on the right-hand side of this equation the value x_2 from the preceding iteration. (In the first iteration the value of x_1 from the preceding point on the contour is taken.) Then, from the now-known x_2 , one calculates $y_2 = f(x_2)$, $\zeta_2 = f'(x_2)$, and from Formula (5) the quantities β_2 (since the entropy s_2 on the contour is known). All the coefficients are determined in the same manner as described for the field points of Fig. 1a. The iterations proceed until sufficient accuracy is achieved. For the control of the accuracy one uses the value of Ψ at point 2 and compares it with the known value of Ψ on the contour.

The evaluation of point 2 on the shock-wave S (Fig. 1c) is achieved by successive estimates of values for the tangent of the shock-angle ξ_2 at this point. Starting from an estimate ξ_2 (close enough to the value at the preceding shock-point O), one determines the following quantities from the shock-equations:

$$\rho_2 = \frac{\lambda_{\infty}^2 \xi_2^2}{1 - \varepsilon \lambda_{\infty}^2 + \xi_2^2} \quad \left(\lambda_{\infty}^2 = \frac{(\kappa + 1) M_{\infty}^2}{2 + (\kappa - 1) M_{\infty}^2} \right)$$

$$\beta_2 = \sqrt{\frac{\lambda_{\infty}^2 (\xi_2^2 + \rho_2^2) - \rho_2^2 (1 + \xi_2^2)}{-\varepsilon \lambda_{\infty}^2 (\xi_2^2 + \rho_2^2) + \rho_2^2 (1 + \xi_2^2)}}, \quad \zeta_2 = \frac{\xi_2 (\rho_2 - 1)}{\xi_2^2 + \rho_2}$$

$$s_2 = \ln \left\{ \left[\frac{2}{\kappa + 1} \frac{\lambda_{\infty}^2 \xi_2^2}{1 + \xi_2^2} - \frac{\kappa - 1}{2\kappa} (1 - \varepsilon \lambda_{\infty}^2) \right] \rho_2^{-\kappa} \right\}$$

and the coordinates x_2 , y_2 from Formula (4), using $\bar{n} = 1/2(\xi_0 + \xi_2)$ instead of n , and approximating the segment of the shock-curve by a parabola. Verification of the correctness of the estimated value of ξ_2 is obtained through the equation along the characteristic of the first family:

$$\zeta_2 - \zeta_1 + K(\beta_2 - \beta_1) + L(y_2 - y_1) - P(s_2 - s_1) = 0$$

The evaluation of the unknown functions is completed with

$$\Psi_2 = \Psi_0 + \kappa \frac{1}{\kappa - 1} \frac{\lambda_{\infty}}{2(1 + j)} \left(\exp \frac{s_0}{\kappa - 1} + \exp \frac{s_2}{\kappa - 1} \right) (y_2^{1+j} - y_0^{1+j})$$

The supersonic parts of flow fields around a series of blunted two-dimensional and axisymmetric bodies of simple shape at zero angle of attack were computed by the described method of characteristics. The blunted wedges and cones had half vertex angles δ of 0, 20, 30, and 40 degrees, and the blunted contours were circular. The two-dimensional bodies were computed at $M = 3, 4$, and 5, and the axisymmetric bodies at $M = 3, 4, 6, 10$ and ∞ . For these cases, the whole flow field was constructed, and in particular the shock-shapes and the pressure distributions on the bodies were obtained. The coefficient of wave-drag c_x , referred to the cross-sectional area of the body, was also determined:

$$c_x = \frac{2(j+1)}{\lambda_{\infty}^2 y^{j+1}} \int_0^y (p - p_{\infty}) y^j dy$$

Some of the results of these computations are presented graphically. Figure 2 displays the flow field around a cone of half-angle $\delta = 20^\circ$ at $M = 6$. In particular, the shock-wave S and the sonic line CD are shown. The computations by the method of characteristics were started on a radial line OB in the supersonic region, on which the initial values were known from the second approximation in the integral method. Only a part of the characteristic net is seen in the figure - actually the segment AB was divided into 48 intervals. In some cases, where a very sharp deceleration of the flow downstream of the transition from the circular to the straight profile was present, successive characteristics of the first family, issuing from this region, did intersect. This fact points to the formation of a "freely hanging" shock-wave in the flow field.

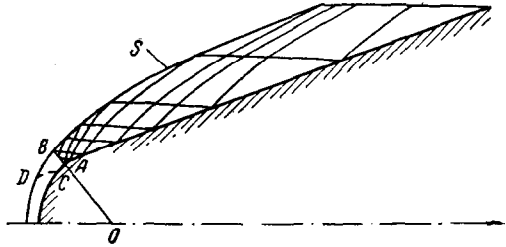


Fig. 2.

At large distances downstream, the shock-wave of the blunted body approaches a conical shock-wave which corresponds to the body without blunting. Figure 3 shows the detached shock-wave for the blunted cone $\delta = 30^\circ$ at $M = 6$. The corresponding conical body and its attached shock are shown as dotted lines for comparison. Also shown is the characteristic of the first family AB , which starts at the juncture between the spherical cap and the conical body and thus separates the purely spherical part of the flow field. If, at B , the shock which corresponds to the spherical cap is weaker than the corresponding cone-shock, the shock-wave of the blunted body will have a point of inflection. Such a case occurs in Fig. 3.

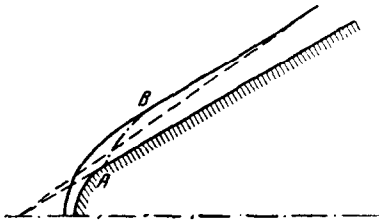


Fig. 3.

At large distances downstream, the shock-wave of the blunted body approaches a conical shock-wave which corresponds to the body without blunting. Figure 3 shows the detached shock-wave for the blunted cone $\delta = 30^\circ$ at $M = 6$. The corresponding conical body and its attached shock are shown as dotted lines for comparison. Also shown is the characteristic of the first family AB , which starts at the juncture between the spherical cap and the conical body and thus separates the purely spherical part of the flow field. If, at B , the shock which corresponds to the spherical cap is weaker than the corresponding cone-shock, the shock-wave of the blunted body will have a point of inflection. Such a case occurs in Fig. 3.

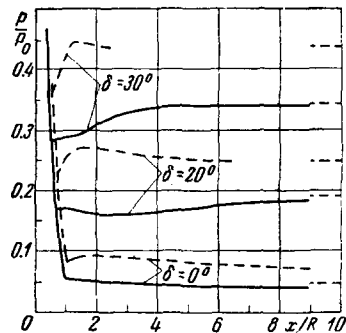


Fig. 4.

The dotted lines in Fig. 4 represent the pressure distributions on blunted wedges and the full lines those on blunted cones with various half-angles δ at $M = 4$. The pressure p is here made dimensionless with the pressure p_0 at the stagnation point and the axial distance x with radius of the blunting contour R . The pressure-curves have two branches - the one on the left corresponds to the circular part of the contour and the one on the right to the rectilinear part of the body. The part of the left branch between the stagnation point and the point where the characteristics method was started is not shown. The corresponding pressure on unblunted wedges and cones is given by the horizontal lines at the right of the figure.

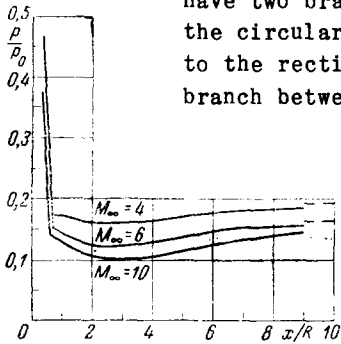


Fig. 5.

The pressure distributions on a cone, $\delta = 20^\circ$, are exhibited in Fig. 5 as functions of M_∞ . Here also the unblunted cone-pressures are shown at the right for the same Mach numbers. It can be seen that on blunted cones at high Mach numbers the pressure continues to fall even on the rectilinear part of the body and that over a sizable part of the body it remains lower than the corresponding pressure on a sharp cone.

The variation of the wave-drag coefficient c_x of the blunted cones $\delta = 0, 20$ and 30° at $M = 6$ with the distance to the base cut-off is displayed in Fig. 6. (The case $\delta = 0^\circ$ refers to a cylinder with a half-sphere for nose.) In the graph, point O corresponds to the stagnation point, for which c_x is simply equal to the pressure-coefficient c_p , and point A to the limit of the region of influence of the nose. The points B_0, B_{20} and B_{30} represent the junctures between the spherical and the straight portions of the body for the respective values of δ .

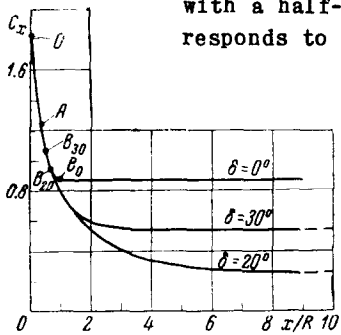


Fig. 6.

Here the dotted horizontal lines indicate the value of c_x on unblunted cones. It is seen that blunting influences the drag of a cone only over a relatively small portion of the body.

Before concluding let us note that the present computations by the method of characteristics were carried out under the author's guidance on the electronic computing machine at the Institute of Numerical Techniques of the Academy of Sciences of the Chinese People's Republic

(Peking). I express by deep appreciation to the Chinese mathematicians Van Shu-Lin, I Chen-Ghuci, Ku Yuan and Len Zun-kai, who set up the programming and carried out the computations on the machine. The author also wishes to acknowledge his indebtedness to O.M. Belotserkovskii and Iu.D. Shmyglevskii for their valuable advice and interest in this work.

BIBLIOGRAPHY

1. Dorodnitsyn, A.A., Ob odnom metode chislennogo reshenia nekotorykh nelineinykh zadach aerogidrodinamiki (On a method of numerical solution of some nonlinear problems of aerohydrodynamics). *Proc. 3rd All-Soviet Mathematical Congress 1956*, Vol. 3, Izd-vo Akad. Nauk SSSR, 1958.
2. Belotserkovskii, O.M., Obtekanie simmetrichnogo profilia s otoshedshei udarnoi volnoi (Flow around symmetric profiles with detached shock waves). *PMM* Vol. 22, No. 2, 1958.
3. Belotserkovskii, O.M., O raschete osesimmetrichnykh techenii s otoshedshei udarnoi volnoi na elektronnoi schetnoi mashine (On the computations of axisymmetric flows with detached shock waves on the electronic computer). *PMM* Vol. 24, No. 3, 1960.
4. Ehlers, F.E., The method of characteristics for iso-energetic supersonic flows adapted to high-speed digital computers. *J. Soc. Industr. and Appl. Math.* Vol. 7, No. 1, 1959. (Russian translation, 1960).
5. Katskova, O.N. and Shmyglevskii, Iu.D., Osesimmetrichnoe sverkhzvukovoe techenie svobodno razshiriaiushchegosia gaza s ploskoi perekhodnoi poverkhnostiu (Axisymmetric supersonic flow of a freely expanding gas with a plane-transitional surface). *Sb. "Vychislitel'naiia matematika" (Collection "Numerical Analysis")*, No. 2. Izd-vo Akad. Nauk SSSR, 1957.

Translated by M. V. M.